Griffey, R. H., Redfield, A. G., Loomis, R. E., & Dahlquist, F. W. (1985) *Biochemistry 24*, 817-822.
Halliday, K. R. (1984) *J. Cyclic Nucleotide Protein Phosphorylation Res. 9(6)*, 435-448.
Manne, V., Bekesi, E., & Kung, H.-F. (1984) *Proc. Natl. Acad. Sci. U.S.A. 82*, 376-380.
McCormick, F., Clark, B. F. C., LaCour, T. F. M., Kjeldgaard, M., Norskov-Lauritsen, L., & Nyborg, J. (1985) *Science 238*, 78-82.
McGrath, H. P., Capon, D. J., Goeddel, D. V., & Levinson, A. D. (1984) *Nature (London) 310*, 644-649.
McIntosh, L. P., Dahlquist, F. W., & Redfield, A. G. (1987a) *J. Biomol. Struct. Dyn. 5*, 21-34.
McIntosh, L. P., Griffey, R. H., Muchmore, D. C., Nelson, C. P., Redfield, A. G., & Dahlquist, F. W. (1987b) *Proc. Natl. Acad. Sci. U.S.A. 84*, 1244-1248.
Mildvan, A. S. (1987) *Magnesium 6*, 28-33.
Nakano, A., Miyazawa, T., Nakamura, S., & Kaziro, Y. (1980) *FEBS Lett. 116*, 72-74.
Nishimura, S., & Sekiya, T. (1987) *Biochem. J. 243*, 313.
Papageorge, A., Lowy, D., & Scolnick, E. M. (1982) *J. Virol. 44*, 509-519.
Pincus, M. R., & Scheraga, H. A. (1985) *Acc. Chem. Res. 18*, 372-379.
Plateau, P., & Gueron, M. (1982) *J. Am. Chem. Soc. 104*, 7310-7311.
Reddy, E. P., Reynolds, R. K., Santos, E., & Barbacid, M. (1982) *Nature 300*, 149-152.
Redfield, A. G. (1986) *NATO ASI Ser., Ser. A 107*, 1-10.
Rosch, P., Whittinghofer, A., Tucker, J., Sczakiel, G., Leberman, R., & Schlichting, I. (1986) *Biochem. Biophys. Res. Commun. 135*, 549-555.
Scolnick, E. M., Papageorge, A. G., & Shih, T. Y. (1979) *Proc. Natl. Acad. Sci. U.S.A. 76*, 5355-5359.
Sigal, I. S., Gibbs, J. B., D'Alonzo, J. S., & Scolnick, E. M. (1986) *Proc. Natl. Acad. Sci. U.S.A. 83*, 4725-4729.
Sweet, R. W., Yoloyama, S., Kamata, T., Feramisco, J. R., Rosenberg, M., & Gross, M. (1984) *Nature (London) 311*, 273-275.
Tabin, C. J., Bradley, S. M., Bargmann, C., Weinberg, R. A., Papageorge, A. G., Scolnick, E. M., Dhar, R., Lowy, D. R., & Change, E. H. (1982) *Nature 300*, 143-149.
Taparowsky, E., Suard, Y., Fasano, O., Shimizu, K., Goldfarb, M., & Wigler, M. (1982) *Nature 300*, 762-765.
Tong, L., de Vos, A. M., Milburn, M. V., Jancarik, J., Noguchi, S., Nishimura, S., Miura, K., Ohtsuka, E., & Kim, S.-H. (1989) *Nature 337*, 90-93.
Trahey, M., Miller, R. J., Cole, G. E., Innis, R. M., Patterson, H., Marshal, C. J., Hall, A., & McCormick, F. (1987) *Mol. Cell. Biol. 7*, 541-544.
Wigler, M., Fasano, O., Taparowsky, E., Powers, S., Kataoka, T., Birnbaum, D., Shimizu, K., & Goldfarb, M. (1984) *Cancer Cells 2*, 419-423.
Willingham, M. C., Pastan, I., Shih, T. Y., & Scolnick, E. M. (1980) *Cell 19*, 1005-1014.
Wittinghofer, A., Goody, R. S., Rosch, P., & Kalbitzer, H. R. (1982) *Eur. J. Biochem. 124*, 109-115.
Yuasa, Y., Srivastava, S. K., Dunn, C. Y., Rhim, J. S., Reddy, E. P., & Aaronson, S. A. (1983) *Nature 303*, 775-779.

Sequence- and Structure-Dependent DNA Base Dynamics: Synthesis, Structure, and Dynamics of Site and Sequence Specifically Spin-Labeled DNA†

Andreas Spaltenstein, Bruce H. Robinson, and Paul B. Hopkins*
Department of Chemistry, University of Washington, Seattle, Washington 98195
Received March 14, 1989; Revised Manuscript Received July 5, 1989

ABSTRACT: A nitroxide spin-labeled analogue of thymidine (**1a**), in which the methyl group is replaced by an acetylene-tethered nitroxide, was evaluated as a probe for structural and dynamics studies of sequence specifically spin-labeled DNA. Residue **1a** was incorporated into synthetic deoxyoligonucleotides by using automated phosphite triester methods. ^{1}H NMR, CD, and thermal denaturation studies indicate that **1a** (T*) does not significantly alter the structure of 5′-d(CGCGAATT*CGCG) from that of the native dodecamer. EPR studies on monomer, single-stranded, and duplexed DNA show that **1a** readily distinguishes environments of different rigidity. Comparison of the general line-shape features of the observed EPR spectra of several small duplexes (12-mer, 24-mer) with simulated EPR spectra assuming isotropic motion suggests that probe **1a** monitors global tumbling of small duplexes. Increasing the length of the DNA oligomers results in significant deviation from isotropic motion, with line-shape features similar to those of calculated spectra of objects with isotropic rotational correlation times of 20-100 ns. EPR spectra of a spin-labeled GT mismatch and a T bulge in long DNAs are distinct from those of spin-labeled Watson-Crick paired DNAs, further demonstrating the value of EPR as a tool in the evaluation of local dynamic and structural features in macromolecules.

Improvements in the synthesis of sequence-defined DNA fragments have made possible the study of sequence-dependent properties of nucleic acids. Both single-crystal X-ray (Wing et al., 1980; Dickerson & Drew, 1981) and nuclear magnetic resonance (Wemmer et al., 1985) studies have revealed a remarkable sequence-dependent structural diversity within B-DNA. The likelihood that this structural variety is important in sequence-dependent recognition phenomena has engendered intense interest in this area. Several lines of evidence have recently suggested that sequence-dependent DNA *dynamics* might likewise be of biological importance. Spe-

† This work was supported in part by grants from the National Science Foundation (PCM-82-16762 and DMB-87-06175), the National Institutes of Health (GM 32681), and the Searle Scholars Program. P.B.H. is an NIH Research Career Development Award recipient (AG 00417).
* Address correspondence to this author.

0006-2960/89/0428-9484$01.50/0

cifically, it has been observed that the affinity of the phage 434 repressor protein dimer for its operator sequence can be reduced 50-fold by changes in the DNA sequence at the center of the operator (Koudelka et al., 1987), despite the failure of the protein to make direct contact with the DNA in this region (Anderson et al., 1987). Indirect experimental evidence that the sequence-dependent deformability of DNA is important in achieving optimal DNA–protein complexation (Hogan & Austin, 1987; Koudelka et al., 1987) has recently been reported (Koudelka et al., 1988). That structural reorganization of DNA can occur as a result of protein binding may be inferred from the finding by single-crystal X-ray analysis that a single synthetic DNA operator adopts different conformations in complexes with 434 repressor and 434 Cro proteins (Wolberger et al., 1988). The goal of the present work is the development of a suitable probe to explore the sequence-dependent dynamics of nucleic acids by using electron paramagnetic resonance spectroscopy.

A variety of techniques have been used for the measurement of DNA dynamics. NMR studies of DNA dynamics of short oligomers have been interpreted in terms of motions spanning a range of at least 10 orders of magnitude (Opella et al., 1981). Most of these studies have addressed very fast, subnanosecond motions in the sugar–phosphate backbone. Base motion has been studied mainly by fluorescence polarization anisotropy (Wahl et al., 1970; Thomas & Schurr, 1983; Ashikawa et al., 1984) and EPR experiments (Bobst et al., 1984; Robinson et al., 1980; Kao & Bobst, 1985; Pauly et al., 1987). Wahl et al. (1970) reported base motion on the nanosecond time scale, based on FAD[1] measurements of ethidium bromide intercalated into DNA. These findings were later interpreted by Barkley and Zimm (1979) as torsional motions about the helix axis. Motions on the 40-ns time scale were likewise detected by Robinson et al. (1980) using EPR spectroscopic measurements of spin-labeled intercalators bound to DNA and were again interpreted as torsional base motions. Unlike the intercalator-based approach to spin labeling of DNA, which is inapplicable to the study of sequence-dependent motion, direct attachment of a spin probe to DNA has been accomplished by Bobst et al. (1984) and Kao et al. (1983), who have prepared several spin-labeled DNAs. In these studies, it was found that the tether which connects the DNA to the nitroxide spin probe has a profound impact on the resulting EPR spectra, longer tethers permitting the probe to undergo significant motion independent of the DNA.

The data were analyzed by using an anisotropic, rigid-body model for the dynamics, involving two characteristic rotational correlation times. The faster of these, found to be tether dependent and always less than 1 ns in DNA (Kao & Bobst, 1985), was attributed to probe motion independent of the attached base, and the longer, a constant ca. 4 ns, to motion of the base. The latter figure is in rough agreement with several NMR studies (Hogan & Jardetzky, 1979; Early & Kearns, 1979; Bolton & James, 1980) involving relaxation measurements, but in disagreement with others (Opella et al., 1981; Allison & Schurr, 1979).

[1] Abbreviations: Ar, aromatic; ATP, adenosine triphosphate; CD, circular dichroism; d, doublet; DMSO, dimethyl sulfoxide; DMT, 4,4′-dimethoxytriphenylmethyl; DTT, dithiothreitol; EDTA, ethylenediaminetetraacetic acid; EI, electron impact; EPR, electron paramagnetic resonance; FAD, fluorescence anisotropy decay; HRMS, high-resolution mass spectrometry; IR, infrared; LRMS, low-resolution mass spectrometry; m, multiplet; MRE, mean residue ellipticity; NMR, nuclear magnetic resonance; p-Tol, *p*-toluoyl; PAGE, polyacrylamide gel electrophoresis; s, singlet; TLC, thin-layer chromatography; t, triplet; UV, ultraviolet.

The disagreement of the conclusions of previous studies has prompted us to develop a new DNA dynamics nitroxide spin probe which (1) can be incorporated into DNA by automated chemical synthesis, thus maximizing options for sequence-dependent studies, and (2) rigidifies the linkage between spin probe and nucleic acid relative to existing probes, with the goal of diminishing or eliminating the need to distinguish motion of the probe from the DNA. We describe here the synthesis and incorporation of probe **1a** into synthetic DNAs. Spectroscopic studies (CD, ^{1}H NMR, and UV-monitored melting) suggest that this probe has only a minor impact on B-DNA; EPR studies reveal probe **1a** to be a considerable improvement over previous spin probes.

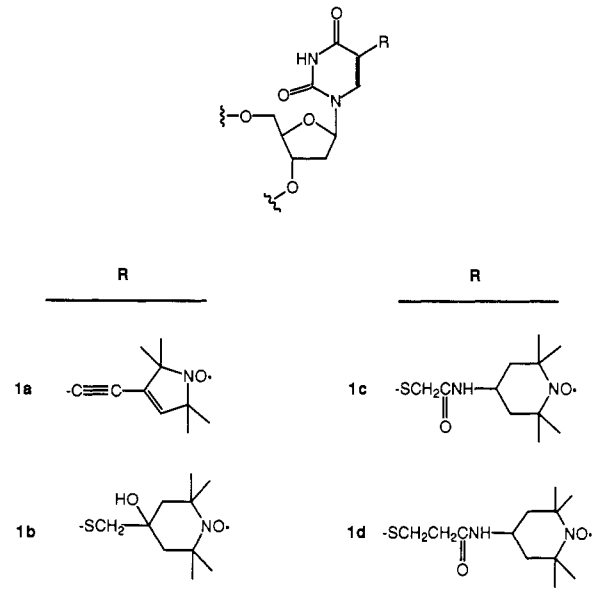

Materials and Methods

Synthesis of Spin Probe **1**: *2,2,5,5-Tetramethyl-3-(2-chloroethenyl)pyrrolidin-1-oxyl* (**2**). (Chloromethyl)triphenylphosphonium chloride (16.6 g, 47.7 mmol) was suspended in 80 mL of tetrahydrofuran, cooled to −78 °C, and treated dropwise with 31.0 mL (43.6 mmol) of 1.37 M *n*-butyllithium in hexanes. The resulting mixture was warmed to −40 °C, stirred for 0.5 h, recooled to −78 °C, and treated with a solution of 2.00 g (11.9 mmol) of 2,2,5,5-tetramethyl-3-formylpyrrolidin-1-oxyl (Hideg et al., 1980) in 20 mL of tetrahydrofuran. The dry ice bath (−78 °C) was then replaced with an ice bath (0 °C), and the mixture was stirred for 0.5 h and quenched with water. The organic layer was dried over magnesium sulfate and concentrated in vacuo. Chromatography on silica gel (25% ethyl acetate–hexanes) afforded 2.19 g (92%) of the vinyl halide **2** as a yellow oil. The product was a mixture of cis and trans isomers (ca. 1:1 by TLC) which were not separated: ^{1}H NMR (500 MHz, $CDCl_3$, phenylhydrazine) δ 1.25 (6 H, s, 2 CH_3), 1.31 (6 H, s, 2 CH_3), 5.60–6.40 (3 H, m, 3 HC=); IR ($CHCl_3$) 3080, 2980, 1610, 1370, 1360 cm^{-1}; LRMS (EI) *m/e* 202 (M^+ + 2, 26), 200 (M^+, 85), 185 ($M^+ - CH_3$), 170 (M^+ − NO), 135 (100); HRMS (EI) calculated for $C_{10}H_{15}NOCl$ 200.0842, observed 200.0842; EPR (acetone) 3 lines.

2,2,5,5-Tetramethyl-3-ethynylpyrrolidin-1-oxyl (**3**). A solution of 2.35 g (23.2 mmol) of diisopropylamine in 50 mL of tetrahydrofuran was cooled to 0 °C and treated with 16.9 mL (23.2 mmol) of *n*-butyllithium (1.37 M in hexanes). After 0.25 h, the solution was cooled to −78 °C and the vinyl halide **2** (2.12 g, 10.6 mmol) was added neat. The resulting mixture was warmed to 25 °C over 2 h and quenched with water.

Extraction with ether, drying over magnesium sulfate, concentration in vacuo, and filtration through a plug of silica gel (20% ethyl acetate/hexanes) yielded a 1:1 mixture of the acetylenic hydroxylamine analogue of **3** and nitroxide **3** (TLC analysis). This mixture was dissolved in 200 mL of methanol, a small piece of copper wire was added, and air was passed through the solution for 12 h until all of the material was oxidized to the nitroxide. (Note: Prolonged exposure of **3** to these conditions should be avoided because oxidative coupling of the terminal acetylene function to a 1,3-diyne results.) Concentration in vacuo afforded **3** as a bright yellow solid (1.39 g, 80%): ^{1}H NMR (500 MHz, $CDCl_3$, phenylhydrazine) δ 1.28 (6 H, s, 2 CH_3), 1.33 (6 H, s, 2 CH_3), 3.01 (1 H, s, HC≡C), 5.93 (1 H, s, HC=); IR ($CHCl_3$) 3300 (s), 2980, 1700, 1372, 1362 cm^{-1}; LRMS (EI) *m/e* 164 (M^+), 149 ($M^+ - CH_3$), 134 ($M^+ - NO$), 91 (100); HRMS (EI) calculated for $C_{10}H_{14}NO$ 164.1075, observed 164.1066; EPR (acetone) 3 lines.

Spin-Labeled Thymidine Analogue **4**. A solution of 0.125 g (0.76 mmol) of the acetylenic nitroxide **3** and 0.400 g (1.13 mmol) of 5-iodo-2′-deoxyuridine in 5 mL of *N*,*N*-dimethylformamide was deoxygenated by repeated exposure to vacuum, followed by the addition of argon. Tetrakis(triphenylphosphine)palladium(0) (0.132 g, 0.114 mmol) and copper(I) iodide (0.290 g, 1.53 mmol) were added, and the system was deoxygenated once more. Triethylamine, 0.073 g (0.72 mmol), was added, and the resulting mixture was stirred at 25 °C until the nitroxide starting material was consumed (6 h, TLC analysis). The volatiles were removed in vacuo, and the residue was suspended in 20% methanol/dichloromethane and filtered through a plug of silica gel. Concentration of the mixture in vacuo and chromatography on silica gel (10% methanol/dichloromethane) afforded the thymidine analogue **4** as a yellow gum (0.223 g, 75%): ^{1}H NMR (500 MHz, acetone-d_6, $Na_2S_2O_4$) δ 1.28 (6 H, s, 2 CH_3), 1.32 (6 H, s, 2 CH_3), 2.32 (1 H, m, 2′ or 2″), 2.44 (1 H, m, 2′ or 2″), 3.82 (2 H, m, 5′, 5″), 4.06 (1 H, m, 3′), 5.51 (1 H, m, 4′), 5.56 (1 H, s, HC=), 6.30 (1 H, m, 1′), 8.29 (1 H, s, H6); IR ($CHCl_3$) 3040, 3020, 1720, 1700, 1690, 1268 cm^{-1}; UV (methanol) 238, 246, 276, 296, 312 nm; EPR ($CHCl_3$/MeOH 1:1) 3 lines.

Monoprotected Nucleoside **5**. Spin-labeled compound **4**, 0.875 g (2.2 mmol), was dissolved in 5 mL of dry pyridine. 4,4′-Dimethoxytriphenylmethyl chloride, 0.800 g (2.4 mmol), was added, and the resulting yellow solution was stirred at 25 °C for 2 h. Methanol (3 mL) was added and the mixture was concentrated in vacuo. Chromatography on silica gel (75% ethyl acetate/hexanes, followed by 10% methanol/dichloromethane) furnished the monoprotected diol **5** as a yellow solid (1.233 g, 81% or 86% based on recovered starting material) and 0.070 g of unchanged starting diol: ^{1}H NMR (500 MHz, acetone-d_6, D_2O, $NaHCO_3$, $Na_2S_2O_4$) δ 1.17 (12 H, s, 4 CH_3), 2.34 (1 H, m, 2′ or 2″), 2.52 (1 H, m, 2′ or 2″), 3.38 (2 H, m, 5′, 5″), 3.72 (6 H, s, 2 CH_3O), 4.18 (1 H, m, 3′), 4.58 (1 H, m, 4′), 5.44 (1 H, s, HC=), 6.32 (1 H, m, 1′), 6.9–7.5 (13 H, m, Ar), 8.10 (1 H, s, H6); IR ($CHCl_3$) 3600, 3380, 3060, 2980, 2840, 1700, 1605, 1505, 1360 cm^{-1}; UV (CH_3CN) 234 (29 000), 275 (9600), 306 (11 600) nm (M^{-1} cm^{-1}); EPR (acetone) 3 lines.

Phosphoramidite **6**. To a solution of 0.250 g (0.36 mmol) of the monoprotected diol **5** and 0.040 g (0.24 mmol) of diisopropylammonium tetrazolide in 2.5 mL of dichloromethane at 25 °C was added 0.131 g (0.44 mmol) of bis(diisopropylamino)(2-cyanoethoxy)phosphine. The solution was stirred for 2 h at 25 °C, partially concentrated in vacuo, and loaded onto a silica gel column. Rapid elution (argon pressure) with 75% ethyl acetate/hexanes, followed by lyophilization from benzene, afforded phosphoramidite **6** as a pale yellow, voluminous solid (0.249 g, 77%): ^{1}H NMR (500 MHz, $CDCl_3$, phenylhydrazine) δ 1.00–1.45 (24 H, m, 8 CH_3), 2.2–2.5 (4 H, m, 2′, 2″, CH_2CN), 3.2–3.7 (4 H, CH_2O, 5′, 5″), 3.78 (6 H, s, 2 CH_3O), 4.15 (1 H, m, 3′), 4.55 (1 H, m, 4′), 5.31 and 5.37 (1 H, 2 s, ratio 1:1, HC=), 6.32 (1 H, m, 1′), 6.8–7.4 (13 H, m, Ar), 8.01 and 8.08 (1 H, 2 s, ratio 1:1, H6); ^{31}P NMR (121 MHz, C_6D_6) δ 153.2 and 153.7; IR ($CHCl_3$) 3380, 3080, 3060, 2980, 1700, 1605, 1505, 1362 cm^{-1}; UV (CH_3CN) 234 (24 500), 275 (9200), 303 (10 400) nm (M^{-1} cm^{-1}); EPR (acetone) 3 lines; MS (FABS, 3-nitrobenzyl alcohol matrix) 892 (M^+), 894 ($M^+ + 2$). [Note: The addition (Atkinson et al., 1985) of triethylamine or pyridine to the chromatography solvent to prevent loss of the dimethoxytrityl protective group had adverse effects in this case, leading to extensive loss of the cyanoethyl protecting group.]

Nucleotide **7**. A solution of 0.038 g (0.054 mmol) of alcohol **5** and 0.035 g (0.58 mmol) of tetrazole in 1 mL of dichloromethane was treated at 25 °C with 0.100 g (0.38 mmol) of bis(2-cyanoethoxy)(diisopropylamino)phosphine and stirred for 0.5 h. An excess (0.5 g) of iodosobenzene diacetate was then added, and the resulting solution was stirred for 0.5 h. The volatiles were removed, and the residue was dissolved in 5 mL of concentrated aqueous ammonium hydroxide. After being warmed to 50 °C, the mixture was concentrated and the resulting gum was dissolved in 80% aqueous acetic acid. After 12 h, the mixture was concentrated to dryness and chromatographed twice by preparative TLC (60% methanol/dichloromethane and 50 mL of methanol/50 mL of dichloromethane/30 drops of concentrated aqueous ammonium hydroxide) to afford the 3′-phosphorylated spin-labeled thymidine analogue **7**: ^{1}H NMR (D_2O, ascorbic acid, 500 MHz) δ 1.65 (6 H, s, 2 CH_3), 1.70 (6 H, s, 2 CH_3), 2.55 (1 H, m, 2′ or 2″), 2.75 (2 H, m, 2′ or 2″), 3.7–3.95 (2 H, m, 5′, 5″), 4.25 (1 H, m, 3′), 6.35 (2 H, s, 1′ and =CH), 8.45 (1 H, s, H6); UV (water) 223 (7100), 231 (6800), 247 (7100), 259 (7600), 274 (7000), 302 (9200) nm (M^{-1} cm^{-1}); EPR [pH 7.0 buffer (100 mM NaCl, 10 mM PO_4^{3-}, 0.1 mM EDTA)] 3 lines.

Enzymatic Ligations. Crude 5′-phosphorylated GCGAATT*CGCGCGCGC (40 OD_{260}) was treated with 40 units of T4 DNA ligase (BRL) in 40 mL of buffer (250 μM Tris/100 mM $MgCl_2$/10 mM DTT/4 mM ATP, pH 7.8). After 48 h at 37 °C, 300 μL of formamide was added, and the resulting mixture was loaded onto a 20% denaturing polyacrylamide gel. Electrophoresis resulted in a ladder of bands (UV visualization) presumably corresponding to 32, 48, 64, 80, 96, and >96 bp fragments. Bands were cut from the gel, crushed, and soaked with buffer (10 mM Tris, 1 mM EDTA, pH 7.4). The supernatant was desalted on a reversed-phase Seppack-18 column (rinse with 10 mL of 10 mM ammonium acetate, elution of DNA with 25% acetonitrile/water) to afford ca. 1–2 OD_{260} of each fraction.

Oligonucleotide Synthesis. The oligomers used in this study were synthesized by using the solid-phase phosphoramidite protocol on an Applied Biosystems Model 380A DNA synthesizer. The synthesis cycle used was detritylation (1% trichloroacetic acid, 1 min), coupling (0.1 M tetrazole in acetonitrile, 1 min), capping (2 M acetic anhydride in THF and 2 M 1-methylimidazole in THF, 0.5 min), and oxidation (0.03 M iodine in pyridine/water/THF, 2 min). Unless otherwise specified, synthetic oligomers possessed both 3′- and 5′-hydroxyl functions. Cleavage from the resin was accomplished with 4 portions of concentrated aqueous ammonium hydroxide

Scheme I

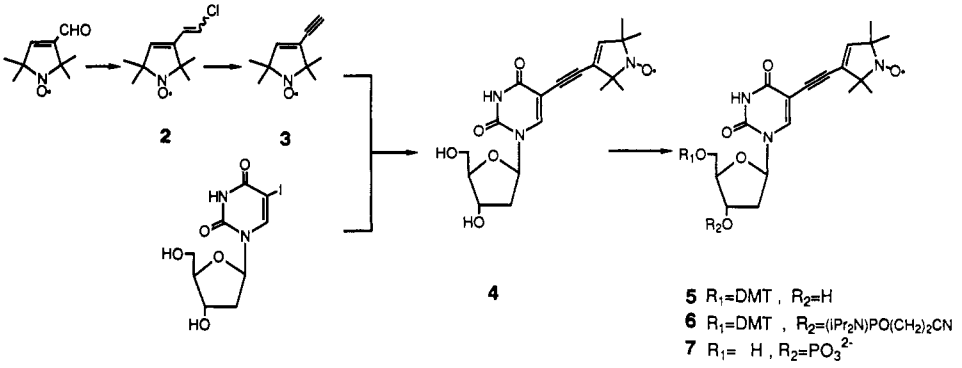

for 15 min each. Removal of the amide-protecting groups was achieved by heating the decanted ammoniacal solution at 55 °C for 15 h. The crude oligomers were then purified by denaturing polyacrylamide gel electrophoresis (see above), eluted from the crushed gel slices with 3 portions of buffer (10 mM Tris, 1 mM EDTA, pH 7.4) for 5 h each, and desalted on a reversed-phase cartridge Seppack-18 (elution with 25% acetonitrile/water). Final purification of the samples was accomplished by gel filtration on Sephadex G-15. Elimination of the latter step afforded EPR spectra containing a subnanosecond component, due to the presence of the aglycon of **1a** which resulted from thermally induced depyrimidination of the spin-labeled base during the sample recovery from gel electrophoresis. This was confirmed by heat treatment of the diol **4** in pH 7 buffer (10 mM PO_4^{3-}, 100 mM NaCl, 0.1 mM EDTA) at 90 °C for 6 h, which resulted in quantitative conversion into two new compounds (TLC analysis) which were isolated by preparative TLC. The more polar compound (lower R_f on TLC) was identified as 2-deoxyribose by comparison with a commercial sample (500 MHz ^{1}H NMR, TLC) and the less polar material as the aglycoside of **4** (UV, 500 MHz ^{1}H NMR, HRMS, and EPR).

EPR Spectra. Continuous-wave EPR spectra were recorded as described previously (Mailer et al., 1985) and, unless specifically indicated otherwise, were obtained in pH 7.0 buffer (100 mM NaCl, 10 mM PO_4^{3-}, 0.1 mM EDTA) at DNA concentrations of ca. 0.1 mM of single strand and at 0 °C.

CD Spectra. CD spectra were recorded on a Jobin Yvon Dichrograph Mark III instrument at ambient temperature with a path length of 1 mm. Samples were dissolved in pH 7.0 buffer (100 mM NaCl, 10 mM PO_4^{3-}, 0.1 mM EDTA) at ca. 0.2 mM in single strand.

UV Melting Profiles. UV-monitored thermal denaturation experiments were conducted by using a Hitachi 100-80 UV spectrophotometer connected to a Haake KT2 thermostated water bath. The temperature was increased at a rate of 0.5 °C/min. Samples were 4–20 μM in single strands in pH 7.0 buffer (100 mM NaCl, 10 mM PO_4^{3-}, 0.1 mM EDTA).

NMR of Exchangable Protons. ^{1}H NMR spectra of imino protons were determined on a Bruker WM 500 instrument, with samples of ca. 0.25 mM of duplex DNA in aqueous sodium phosphate buffer (100 mM NaCl, 10 mM PO_4^{3-}, 0.1 mM EDTA) containing 10% D_2O, at pH 7.0. Peak suppression of the water resonance was achieved by the method of Redfield et al. (1979).

Results

Design and Synthesis of Probe **1a**

Design. Bobst and co-workers (Bobst et al., 1984, 1988; Kao & Bobst, 1985; Pauly et al., 1987) have incorporated a variety of spin-labeled bases into DNA using enzymatic methods. Structures **1b–d** are representative of these structures, all of which bear the label in the major groove, where the chances of structural disruption are minimized. In one study, tethers ranging in length from 2 to 6 atoms were employed to connect the uracil base to the piperidinyloxy spin label (Bobst et al., 1984). It was observed that the shortest of these tethers (**1b**) in duplex DNA afforded EPR spectra consistent with the slowest overall motion of the probe. The slowest component of these spectra remained in the 4-ns correlation time range, however, considerably faster than that seen in studies using FAD (Wahl et al., 1970) or EPR of DNA-bound intercalators (Robinson et al., 1980). For this reason, we have extended this series by synthesizing the precursor for incorporation of residue **1a** into DNA.

Probe **1a** does not entirely eliminate the possibility of nitroxide motion independent of the DNA. While probe **1a** is expected to have only slight conformational mobility of the five-membered, unsaturated nitroxide-bearing ring, the acetylene linkage offers the possibility of rotation of this ring independent of the heterocyclic base to which it is attached. Space-filling, CPK models of **1a** in B-DNA suggested that the latter rotation might be hindered, or even precluded, by collision of the methyl substituents of the five-membered ring with the proximal wall of the major groove.

To take maximal advantage of a nitroxide spin probe in the study of sequence-dependent DNA dynamics, we have prepared **1a** in a protected form useful in automated chemical synthesis. This approach not only allows the convenient synthesis using current technology of micromole quantities of up to roughly 100-base oligonucleotides of any sequence but also in conjunction with enzymatic ligation provides access to DNAs with virtually any desired size or sequence characteristics.

Synthesis. Scheme I outlines the synthesis of the spin-labeled phosphoramidite **6** required for the incorporation of residue **1a** into synthetic DNA. The known aldehyde 2,2,5,5-tetramethyl-3-formylpyrrolidin-1-oxyl (Hideg et al., 1980) was converted to vinyl halide **2** (1:1 mixture of cis and trans). Dehydrohalogenation with lithium diisopropylamide at −78 °C afforded the acetylenic nitroxide **3**. Palladium-mediated coupling (Robins & Barr, 1983) with 5-iodo-2′-deoxyuridine produced the thymidine analogue **4** in good yield. Selective protection of the 5′-OH and phosphorylation of the 3′-OH produced the spin-labeled phosphoramidite **6**.

Control experiments using diol **4** demonstrated that the spin-labeled heterocycle was stable to all of the reagents and conditions required for phosphite triester, solid-phase DNA synthesis (Letsinger & Lunsford, 1976; Beaucage & Caruthers, 1981), with the single exception of treatment with thiophenol, the reagent commonly employed for removal of the phosphate methyl ester that results when methyl is chosen

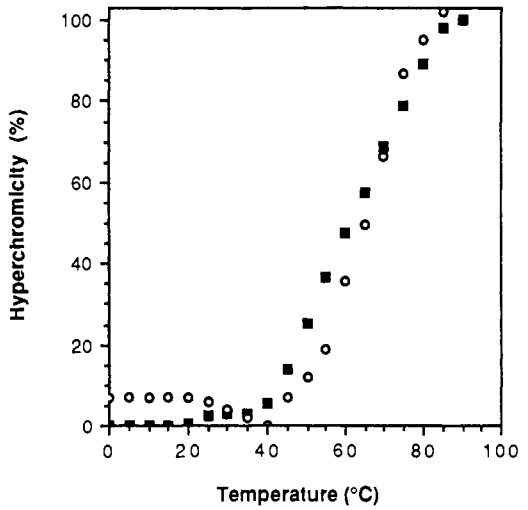

FIGURE 1: Thermal denaturation of CGCGAATTCGCG duplex (■) and CGCGAATT*CGCG (○) monitored at 260 nm (ca. 2 μM in duplex, 100 mM NaCl, 10 mM phosphate buffer, pH 7.0, 0.1 mM EDTA).

as the phosphorus protective function. For this reason, β-cyanoethyl protection was chosen. Automated DNA synthesis was then achieved by standard methods, the resulting oligonucleotide being purified by sequential PAGE, by desalting on a reverse-phase column, and finally by size exclusion chromatography on Sephadex G-15.

Structural Characterization of a Spin-Labeled Dodecamer

The self-complementary sequence 5′-d-(CGCGAATT*CGCG), T* = **1a**, was chosen for structural comparison with the native, unlabeled substance (Spaltenstein et al., 1988). This dodecamer duplex, which contains the recognition site for the restriction enzyme *Eco*R1, was selected for several reasons. In addition to extensive X-ray analysis (Dickerson et al., 1982), the dodecamer has previously been characterized by ^{1}H NMR (Hare et al., 1983), CD, UV-melting profiles, and calorimetric methods (Patel et al., 1982a,b; Pardi et al., 1983; Seela & Kehne, 1987).

The UV spectrum of the spin-labeled dodecamer shows a pronounced absorbance beyond the cutoff of the unlabeled dodecamer at roughly 300 nm, consistent with the contribution of the modified base **1a**, which has λ_{max} at 305 nm (measured by using **4**). The presence of residue **1a** likewise has an impact on the CD spectrum of the spin-labeled dodecamer duplex (Spaltenstein et al., 1988). The contribution of residue **1a**, modeled by using the CD spectrum of **7**, accounts at least qualitatively for the diminished mean residue ellipticity of the ca. 280-nm maximum relative to the unlabeled duplex. The CD spectrum of the labeled dodecamer is consistent with its existence as a duplex.

UV-monitored thermal denaturation profiles for the labeled (**1a**) and unlabeled dodecamer duplexes (Figure 1) exhibited similar cooperativity and midpoint of the melting transition, offering further support for the nondisruptive character of the spin probe on the duplex structure.

The imino region of the ^{1}H NMR spectra of the spin-labeled (**1a**), native, and spin-labeled (**1a**)/reduced dodecamer duplexes reveal four of the five observed resonances to have nearly identical chemical shifts in the labeled and unlabeled duplexes (Figure 2). The indicated resonance assignments in the native dodecamer are after Patel et al. (1982b); the labeled strand resonances were assigned by analogy with the additional assumption that the shifted resonance ($\Delta\delta$ 0.65 ppm) is that of

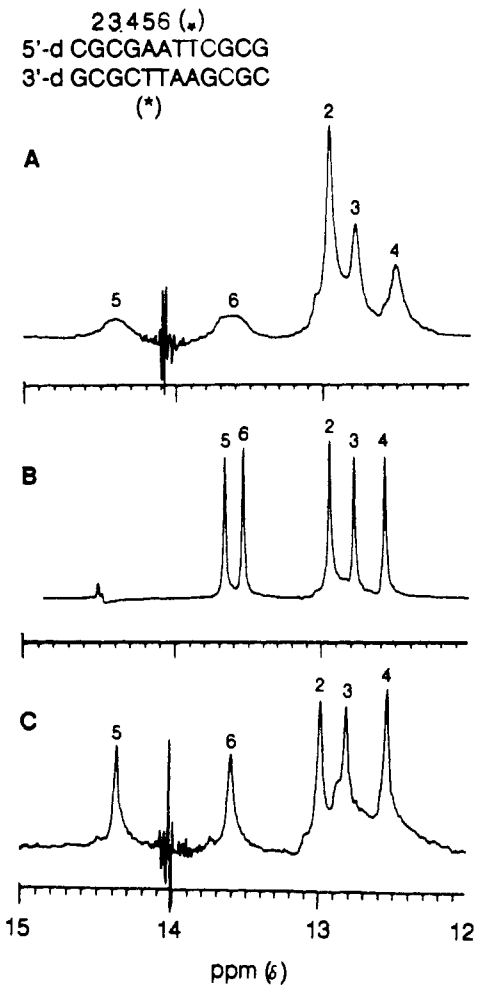

FIGURE 2: ^{1}H NMR spectra (500 MHz) of the imino region of (A) CGCGAATT*CGCG, (B) CGCGAATTCGCG, and (C) CGCGAATT*CGCG after treatment with $Na_2S_2O_4$ (100 mM NaCl, 100 mM phosphate buffer, pH 7.0, 0.1 mM EDTA, 10% D_2O, 20 °C, 250 μM duplex DNA). The origin of the artifacts (14 ppm in A and C, 14.5 ppm in B) observed in all spectra is unknown.

the spin-labeled residue. This interpretation is supported by the downfield shift in **4** relative to thymidine of the NH resonance by 0.5 ppm in DMSO-d_6. A similar effect has been observed recently in 5-fluorodeoxyuridine-containing oligomers (Kremer et al., 1987; Sowers et al., 1987). The nitroxide causes extensive distance-dependent spin relaxation manifested by the broadening of the resonances closest in space to the spin label. Distance geometry calculations based on line-width measurements (data not shown) for the imino protons are qualitatively consistent with the expected location of the imino protons in a double-helical duplex. Upon reduction of the nitroxide with sodium dithionite, the distance-dependent line broadening was eliminated. Although we do not currently know the origin of a minor residual line broadening (11 Hz) relative to the unlabeled duplex, we note that residual unreduced nitroxide, sodium dithionite, or some other spin could be responsible.

EPR Spectra of Spin-Labeled Duplex DNAs

EPR Spectra of Dodecamer and Tetraeicosamer Duplexes. The EPR spectra of three duplexes spin labeled with **1a** are shown in Figure 3. These include two dodecamers [(CGCGAATT*CGCG)$_2$ and $T_5T^*T_6{\cdot}A_{12}$] and a tetraeicosamer (24-mer, GGCGCGGATAATT*CGTGCCGGCGT·ACGCCGGCACGAATTATCCGCGCC). These spectra demonstrate the length dependence of the EPR spectra of

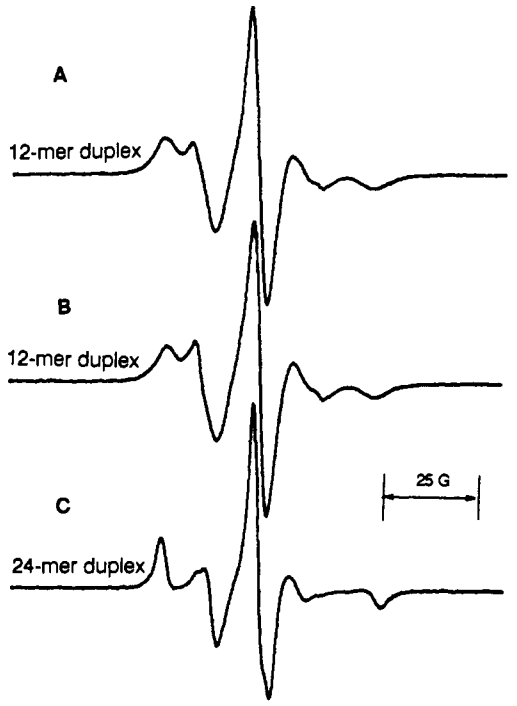

FIGURE 3: EPR spectra of (A) $T_5T^*T_6{\cdot}A_{12}$, (B) $(CGCGAATT^*CGCG)_2$, and (C) GGCGCGGATAATT*CGT-GCCGGCGT·ACGCCGGCACGAATTATCCGCGCC (ca. 60 μM duplex DNA, 100 mM NaCl, 10 mM phosphate buffer, pH 7.0, 0.1 mM EDTA, 0 °C).

Table I: Rotational Correlation Times Calculated for a Right-Circular Cylinder for Motion About ($\tau^2_{\pm 2}$) and Perpendicular to (τ^2_0) the Helix Axis

no. of base pairs of duplex DNA	τ^2_0 (ns)	$\tau^2_{\pm 2}$ (ns)
12	14.3	8.9
24	54.5	17.8
150	4503.3	107.5

duplexes bearing **1a**, the two dodecamers affording virtually identical spectra and the tetraeicosamer spectrum being clearly distinct.

The EPR Spectra of Short Spin-Labeled Duplexes Are Dominated by Global Molecular Tumbling. Interpretation of the EPR spectra of spin-labeled DNA is complicated by the anisotropic nature of the molecular motions which determine the spectra. These potentially include movement of the probe independent of the base to which it is attached, motion of the spin-labeled base relative to the macromolecule, and tumbling of the macromolecule. The DNA length dependence of the EPR spectra in Figure 3 suggests that the first of these, motion of the probe **1a** independent of the nucleic acid, does not dominate the EPR signal and suggests that base motion and/or global molecular tumbling may be responsible for the spectra. On the basis of the assumption that short duplex DNAs have the shape of a right-circular cylinder, hydrodynamic theory can be used to estimate the rotational correlation times for tumbling of the duplex parallel to ($\tau^2_{\pm 2}$) and perpendicular to (τ^2_0) the helical axis (Tirado & de la Torre, 1980) in aqueous medium as a function of viscosity and temperature. Under the current conditions (0 °C, 100 mM NaCl), these calculated rotational correlation times are as shown in Table I (see Appendix for details of the hydrodynamic calculations). For the present purposes, it is useful to compare the EPR spectra of the dodecamers and tetraeicosamer to the calculated isotropic calibration spectra characterized by a single effective rotational correlation time (τ_c).

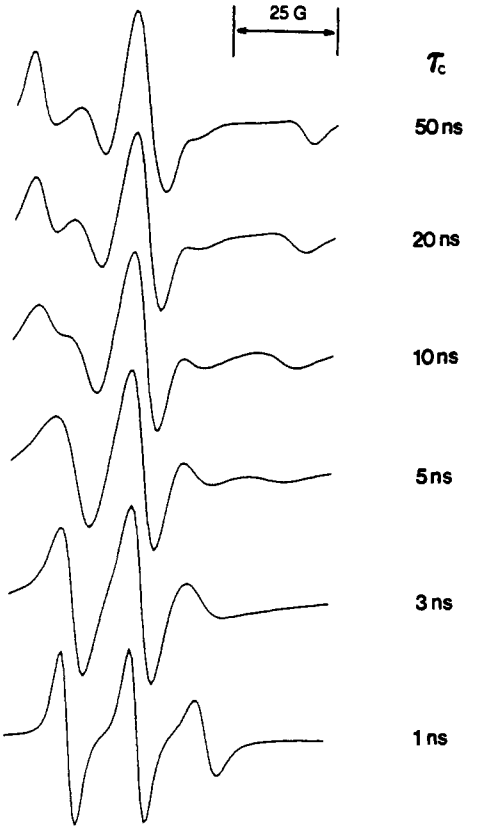

FIGURE 4: Theoretical linear CW EPR spectra calculated assuming isotropic rotational diffusion with the indicated rotational correlation times, τ_c: G_{xx} = 2.0091, G_{yy} = 2.0061, G_{zz} = 2.0020, A_{xx} = 7.000 G, A_{zz} = 35.000 G, $T_{1e} = 3.0 \times 10^{-6}$ s, $T_{2e} = 9.0 \times 10^{-8}$ s. All spectra are convoluted with a 1.5-G gaussian line broadening.

It can be shown that the general line-shape features of the EPR spectrum of a hypothetical, tumbling, rigidly spin-labeled, right-circular cylinder will closely resemble those of isotropic calibration spectra (calculated) characterized by a single effective rotational correlation time which is bracketed by τ^2_0 and $\tau^2_{\pm 2}$ values. Simulated isotropic spectra are illustrated in Figure 4. Remarkably, the line shape observed for the dodecamer duplexes is closest to those calculated with a τ_c of ca. 10 ns and that of the tetraeicosamer with 20 ns, in both cases falling within the range predicted by hydrodynamic theory.

EPR Spectra of Single-Stranded DNA. In contrast to the EPR spectra of duplexes, in which a relatively slow global tumbling is dominant, much faster motion of the probe is indicated in the monomer **7** and the single strand $T_5T^*T_6$ (Figure 5). These spectra are well simulated by using a τ_c of 0.1 and 1.25 ns, respectively (Spaltenstein et al., 1989). In the absence of further studies, it is not possible to interpret these spectra in terms of the relative contribution of motion of the probe independent of the DNA and motion of the base itself.

EPR Spectra of Long Duplexes

Watson–Crick Base-Paired DNA. FAD and EPR studies of DNA-bound intercalators led to the conclusion that a base-dependent characteristic motion on the order of 40 ns is present in large DNAs (Wahl et al., 1970; Robinson et al., 1980). Table I suggests that duplex DNAs larger than roughly 150 bp should undergo global tumbling (assuming the rigid right-circular cylinder model) on a time scale significantly slower than this, and thus, if 40-ns motions are present, they may dominate the resulting EPR spectra of spin-labeled duplexes larger than 150 bp. Spin-labeled DNAs anticipated to be sufficient in size to slow global tumbling and permit

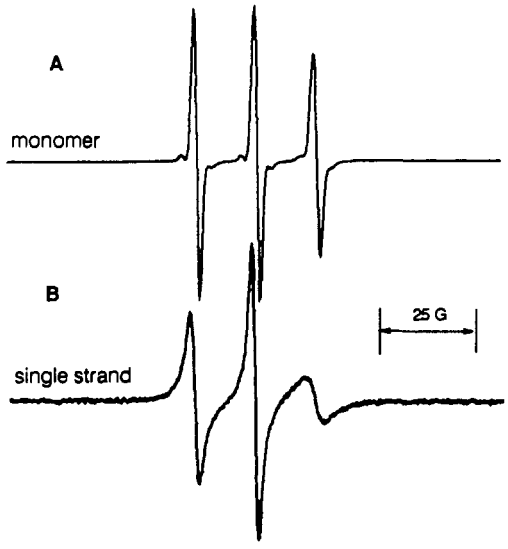

FIGURE 5: EPR spectra of (A) thymidine analogue 7 and (B) TTTTTT*TTTTTT (ca. 150 μM single strands, 100 mM NaCl, 10 mM phosphate buffer, pH 7.0, 0.1 mM EDTA, 0 °C).

observation of local base motion were prepared by two methods. In the first, a spin-labeled homooligomer ($T_{11}T^*T_{12}$) was annealed to an excess of a commercial homopolymer [poly(dA)]. In the second, a series of spin-labeled hexadecamers were designed in which dimerization was expected to afford a 10-base, spin-labeled duplex region with flanking $(CG)_3$ 5′ overhangs. Self-assembly of the overhangs was then expected to produce duplexes of indefinite length bearing periodic gaps in the covalent sugar–phosphate backbone. The EPR spectra of all of these samples (Figure 6) are strikingly similar in their general features and appear to represent homogeneous samples. Simulated spectra which assume isotropic motion do not duplicate these spectra particularly well, suggesting that these spectra are dominated by a distinctly anisotropic motion. The general features of the spectra, particularly the splitting and shapes of the high- and low-field lines, most resemble simulated isotropic spectra with a τ_c in the 20–100-ns range.

To evaluate the impact of the frequency of covalent gaps in the sugar–phosphate backbone, GCGAATT*CGCGCGCGC was synthesized with a 5′-phosphate and ligated by using T4 DNA ligase. Denaturing PAGE afforded a ladder of discrete bands from which homogeneous samples presumably of lengths 32, 48, 64, and 80 residues were obtained. The EPR spectra of these samples, which retain sticky ends and should again self-assemble into larger structures, were virtually identical with that of the 5′-phosphate of the 16-mer (which was not significantly distinct from that of the 3′,5′-diol), indicating that the periodic gaps have little influence on the resulting spectra.

A Long Duplex Bearing a Spin-Labeled GT Mismatch. The sequence GCGGATT*CGCGCGCGC is analogous to a self-assembling sequence described above (GCGAATT*CGCGCGCGC) with the single change that the base-pairing partner of the spin-labeled thymidine residue has been changed from deoxyadenosine to deoxyguanosine. The EPR spectrum of this GT-mismatch-bearing sequence (Figure 7) is distinct from the other long duplexes (Figure 6). Reference to the simulated isotropic spectra (Figure 4) suggests that the probe is in a heterogeneous and significantly more mobile environment than the Watson–Crick base-paired analogue.

A Long Duplex Bearing a Spin-Labeled T Bulge. The sequence GCGT*AATTCGCGCGCGC is analogous to a self-assembling sequence described above (GCGAATT*CGCGCGCGC) with the single change that a spin-labeled thymidine residue which has no base-pairing partner has

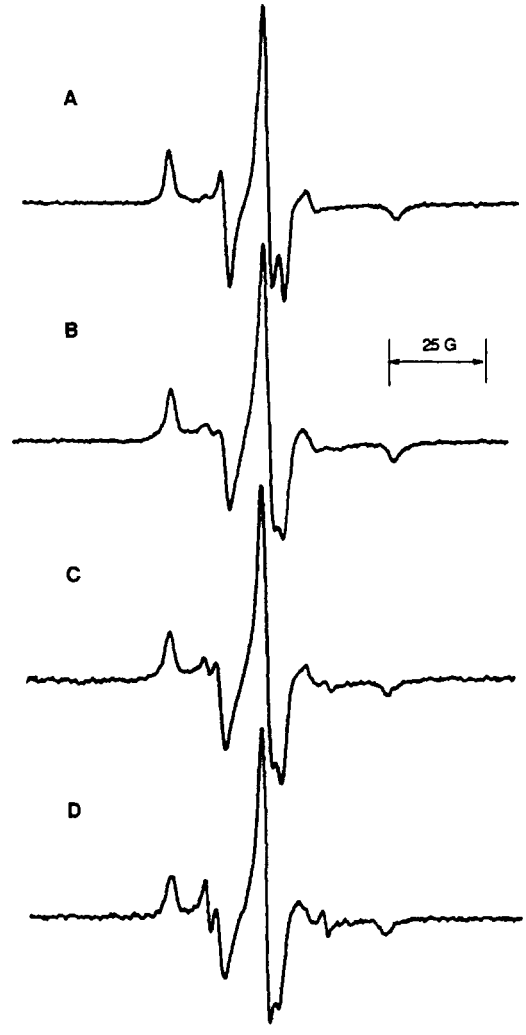

FIGURE 6: EPR spectra of (A) $T_{11}T^*T_{12}$·poly(dA). (B) GCGAATT*CGCGCGCGC, (C) GTAAATT*TACGCGCGC, and (D) GCGAGCT*CGCGCGCGC (ca. 150 μM in labeled strands for A and B, 50 μM for C and D, 100 mM NaCl, 10 mM phosphate buffer, pH 7.0, 0.1 mM EDTA, 0 °C).

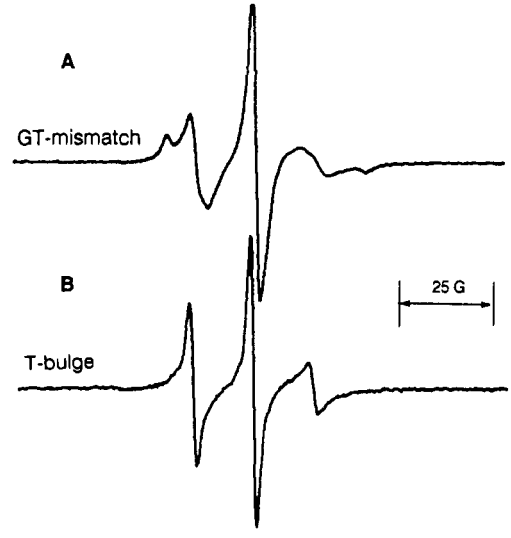

FIGURE 7: EPR spectra of (A) 5′-d(GCGGATT*CGCGCGCGC) and (B) 5′-d(GCGT*AATTCGCGCGCGC) (ca. 150 μM single strand, 10 mM phosphate buffer, pH 7.0, 100 mM NaCl, 0.1 mM EDTA, 0 °C).

been inserted into the sequence. The EPR spectrum of this material (Figure 7) is entirely distinct from the Watson–Crick paired duplexes and is instead similar to that of a highly mobile spin-labeled single strand.

Discussion

Previous studies of spin-labeled DNA have achieved the attachment of the spin label by a variety of methods, the majority of which are practically inapplicable to the study of sequence-dependent dynamics. Methods involving the covalent attachment of spin probe to DNA by the chemical reaction of intact DNAs with reactive spin labels (Dugas, 1977; Kamzolova & Postnikova, 1981) and the noncovalent labeling by incubation of DNA with covalently spin-labeled intercalators (Robinson et al., 1980) are destined to afford a heterogeneous product. More promising is the method of Bobst, in which a spin-labeled nucleoside triphosphate is incorporated during template-directed enzymatic synthesis (Bobst et al., 1988). A sequence specifically spin-labeled duplex 26-mer has been prepared by this method. In this paper, we report the first example of nitroxide spin labeling of DNA using automated, phosphite triester chemistry. This work demonstrates that the chemical steps required for DNA synthesis, which include treatments with acid, base, and oxidation reagents, and purification do not destroy the nitroxide moiety. In combination with enzymatic methods for the incorporation of synthetic oligonucleotides into much larger DNAs, this technology enables, in principle, the sequence-defined spin labeling of DNAs of any size and desired sequence.

On the basis of comparison of native and spin-labeled CGCGAATT*CGCG in duplex form by CD, ^{1}H NMR, and UV-monitored thermal denaturation, the probe **1a** appears not to disrupt the solution structure of B-DNA. A similar conclusion has been reached in the study of a 5-fluorodeoxyuridine-bearing oligonucleotide duplex (Kremer et al., 1987; Sowers et al., 1987). Examination of space-filling, CPK models of right-handed Watson–Crick paired double helices suggests that the spin probe has ample room to reside in the major groove without disruption of any aspect of DNA structure. Models suggest that the acetylene linkage is critical in the latter regard: the tetramethyl substitution pattern which is required for steric protection of the otherwise reactive nitroxide moiety occupies a significant volume, and acetylene acts as a ca. 4-Å spacer between this grouping and the DNA. While minor differences in the spectroscopic properties of the native and spin-labeled dodecamers may reflect structural or dynamic perturbations caused by the spin label, we believe that the body of evidence presented here suggests such effects are minimal. Verification that spin probe **1a** is truly nondisruptive must await a more detailed structural evaluation, for example, by single-crystal X-ray or ^{1}H NMR analysis.

Two duplex DNA 12-mers spin labeled with **1a** afford nearly identical solution EPR spectra. In contrast, the EPR spectrum of an analogously spin-labeled duplex 24-mer is distinct (Figure 3). Comparison of the experimental EPR spectra with simulated spectra representing a single-characteristic isotropic rotational correlation time, τ_c, suggests that the spectrum of the 24-mer is indicative of slower probe motion than the spectra of the two 12-mers. Importantly, the general line-shape features of these spectra are not dominated by the subnanosecond component observed with other less rigid spin probes in indefinitely long, duplex, spin-labeled DNAs (Kao et al., 1983; Bobst et al., 1984; Kao & Bobst, 1985). Furthermore, contrary to the latter studies, we conclude that there is no significant base motion on the 4-ns time scale. It is probable that the assumption which led to the earlier model—that all probe motion independent of the DNA occurs in the plane of the base—is invalid. While we cannot at this time rule out the possibility that probe **1a** acts as an impediment to and thus precludes this fast motion, the more likely interpretation is that the relatively fast motions indicated by EPR spectra obtained with less rigidly tethered spin probes reflect probe motion independent of the base in all directions. Final judgement must, however, be reserved until the sensitivity of probe **1a** to the anisotropic motions of DNA is quantitatively evaluated by computer simulation. Qualitative comparison of isotropic simulated and experimental spectra suggests that global tumbling of these relatively short duplexes, calculated by using hydrodynamic theory to be in the 10–20-ns τ_c range (see Appendix), dominates the spectra. Such a finding is consistent with existing quantitative models of DNA base motion which assume that internal motion is dominated by length-dependent, coupled torsional motions (Barkley & Zimm, 1979; Robinson et al., 1980; Allison & Schurr, 1979). For DNAs in the 12–24-bp range, these motions are expected to be of limited significance relative to global tumbling. Consistent with this model is the observation that solutions of spin-labeled 3′-mononucleotide and single-stranded DNA afford EPR spectra (Figure 5) diagnostic for relatively isotropic and rapid (0.1 and 1.25 ns, respectively) motion (Spaltenstein et al., 1989).

The EPR spectra of self-assembling DNA sequences labeled with spin probe **1a** (Figure 6) are indicative of the slowest motions yet observed with covalently spin-labeled DNA. We attribute this to the rigidity of the tether which connects the nucleic acid to the spin label. The quantitative evaluation of these spectra is a subject of current study, but at this time comparison to simulated isotropic spectra allows qualitative discussion. Particularly with respect to line shape, the spectra of these multimers suggest probe motion with a characteristic rotational correlation time (τ_c) of 20–100 ns and lack motion in the 3–20-ns range. Whether the experimental spectra reflect motion of the spin probe independent of the DNA—for example, limited rotation about the acetylene linkage—is currently unknown. Examination of CPK models of duplex DNA bearing **1a** leads to the prediction that rotation about the acetylene axis will be limited by collision of the methyl groups of the nitroxide-bearing ring with the wall of the major groove formed by the spin-labeled strand. Sequence-dependent structural variation impossible to evaluate at this time might, however, render this effect inoperative. It is encouraging that the 20–100-ns time scale is in line with the 40-ns observation using FAD and EPR of intercalator-bound DNA. Furthermore, the similarity of these values using the ostensibly structurally nondisruptive spin probe **1a** and a highly disruptive intercalator offers support that the involved motions are not highly localized and constitute long-range, coupled motions of the polymer. It remains to be seen to what degree motion of the nitroxide of **1a** independent of the DNA influences these spectra of large DNAs.

An unexpected conclusion of this study is that the EPR spectra of spin-label duplex DNAs containing covalent gaps—omission of the phosphate bridge, resulting in 3′ and 5′ alcohol termini—are not appreciably influenced by the frequency of gaps in the range of 1 per 16 base pairs to 1 per 80 base pairs. If these gaps acted as joints capable of flexing on the nanosecond time scale, the EPR spectra would likely be sensitive to this. It is possible that a favorable stacking interaction is responsible for maintaining structural and dynamic continuity at the gap site. A similar invariance of certain dynamic properties to covalent breaks, but at much

lower frequency (1 per 413 base pairs), has been observed for nicked duplex DNA (Thomas et al., 1980).

We have previously reported that the sensitivity of probe **1a** to the dynamic differences of various structural environments has application in the study of DNA structures. This "reporter group" approach may be particularly advantageous when a local feature of structural interest is present in a large DNA. In earlier studies, it was shown that **1a** readily distinguishes hairpin from duplex regions of DNA (Spaltenstein et al., 1989). In the present work, we have spin labeled a GT mismatch (GCGGATT*CGCGCGCGC) and a bulged T (GCGT*AATTCGCGCGCGC) in sequences expected to self-assemble into duplexes of indefinite length. Both of these spectra (Figure 7) are distinct from long spin-labeled Watson–Crick paired duplexes (Figure 6).

DNAs containing mismatched bases are of interest as intermediates in one mechanism of mutagenesis. Previous structural studies, particularly by single-crystal X-ray analysis, have indicated that a variety of mismatches, even the purine–purine pairing, are accommodated by the double helix with quite minimal disruption (Hunter et al., 1987a,b; Brown et al., 1986). The GT mismatch destabilizes duplex DNA by at most a few kilocalories per mole relative to the correctly paired analogues (Aboul-ela et al., 1985; Salisbury & Anand, 1985) and has been shown by both X-ray (Hunter, 1987b) and ^{1}H NMR (Patel et al., 1982c) studies to involve a wobble pairing in which the thymine residue is translated into the major groove and the guanine residue into the minor groove. There is little reason to believe that this modification should have a profound impact on the dynamics of the resulting duplex. Remarkably, the spin-labeled mismatch is entirely distinct in the EPR from the analogous Watson–Crick paired material. The spectrum is distinct from that of a single strand (Figure 5) and is indicative of slower motion arguing against the hypothesis that the sequence has failed to assemble into a duplex structure. It may be that this substance exists in a hairpin or dimeric "dumbell" form with two GATT loops and a 12-bp central duplex (Wemmer & Benight, 1985; Erie et al., 1987). Alternatively, it is possible that the sequence has assembled into an indefinite duplex but that the wobble pairing has reduced constraints on the motion of the spin probe independent of the base. Finally, it is conceivable that a major dynamic difference exists between Watson–Crick and other base pairs, a finding which could have important implications in the recognition of mismatches during the repair process (Loeb & Kunkel, 1982). The two-component appearance of the EPR spectrum of this mismatch suggests that no single explanation will suffice. Regardless of the correct explanation, EPR provides a straightforward method for detecting unusual features in DNA structure and dynamics.

A second example of DNA structures of interest in the mutation process is that of unpaired bases, so-called bulges, which may lead to frame-shift mutation (Streisinger et al., 1966). Structural studies of bulges by ^{1}H NMR and single-crystal X-ray analysis (Miller et al., 1988) have concluded that unpaired bases may be accommodated in either an intra- or extrahelical fashion (van den Hoogen et al., 1988; Kalnik et al., 1989), the determining factors remaining unresolved. The sequence GCGT*AATTCGCGCGCGC affords an EPR spectrum (Figure 7) which is quite similar to that of a single strand (Figure 5). We have observed that even spin-labeled random-sequence DNAs, particularly those which are relatively G-rich, afford spectra indicative of slower motion than that observed for this sequence, presumably due to formation of heterogeneous aggregates. It seems likely that in this case the extended duplex is formed but that the spin-labeled base adopts an extra-helical, single-strand-like environment.

We have demonstrated here that a nitroxide spin probe can be incorporated into synthetic DNA oligomers of any desired sequence using the phosphite triester method. The probe is not appreciably disruptive of duplex DNA structure in the one case studied in detail. The EPR spectra of Watson–Crick base-paired, right-handed duplex structures are sensitive to the size of the macromolecule, consistent with global molecular tumbling at relatively small duplex sizes and local motion of the probe faster than global tumbling in larger duplex sizes. At this time, the degree to which the EPR spectra of spin-labeled large DNAs are influenced by motion of the probe independent of the attached base is unknown and is under investigation. The EPR spectra of duplex DNA, which is disrupted by such features as mispairing or the absence of a pairing partner, are readily distinguished from the Watson–Crick pairing. As such, this spin probe can serve as a probe of DNA structure as well as dynamics. Overall, probe **1a** is well suited to serve as a probe for the sequence-dependent dynamics of nucleic acids.

Acknowledgments

J. Beltman, Dr. F. Miyake, and M. Tippie made significant contributions to the early stages of this work. We thank E. Hustedt and J. Kirchner for numerous and ongoing contributions to this project. We also thank Dr. S. Benight, P. Flynn, G. Parraga, and S. Ribeiro for technical assistance and Drs. M. Caruthers, B. Reid, N. Seeman, and J. M. Schurr for helpful discussions.

Appendix: Estimation of τ_c of Oligomers

As pointed out in the introductory paragraphs, DNA duplexes similar in size to the ones used in our studies (10–30 bp) can be approximated by a freely tumbling cylindrical object. Given below is a set of equations which permits the calculation of an estimate for the expected correlation time for a duplex of given length. Separate values are obtained for the movement perpendicular and parallel to the principal axis of rotation. The equations given are those derived by Tirado and de la Torre (1980) for the diffusion coefficients of a right-circular cylinder of radius R and length L. For rotation around an axis perpendicular to the axis of cylindrical symmetry, the rotational diffusion coefficient is given by

$$D_{perp} = \frac{[\ln (p) + \delta_1] \times 3kT}{\pi\eta L^3} \qquad \text{(A-1A)}$$

For motion around the axis of cylindrical symmetry, the rotational diffusion coefficient is given by

$$D_{para} = \frac{kT}{(1 + \delta_2)A\pi\eta LR^2} \qquad \text{(A-1B)}$$

where η is the viscosity of the medium; $p = (L/2R)$ is the length-to-diameter ratio; k is Boltzmann's constant; and T is the temperature in kelvin.

δ_1, δ_2, and A are given in tabular form by Tirado and de la Torre (1980). A equals 3.841 and is a constant. We have parameterized the tabular data of Tirado and de la Torre (1980) for the dependence of δ_1 and δ_2 on p and find

$$\delta_1 = -0.661 + 0.891(p^{-1}) \qquad \text{(A-2A)}$$

and

$$\delta_2 = 0.688(p^{-1}) - 0.202(p^{-2}) \qquad \text{(A-2B)}$$

Spectra were recorded at 0 °C in 10 mM phosphate buffer

and 100 mM NaCl; therefore, $\eta = 0.01796$ g cm^{-1} s^{-1} (corresponds to 120 mM NaCl solution at 0 °C); $k = 1.38063$ g cm^2 K^{-1} s^{-2}; $T = 273$ K; and $\pi = 3.1416$.

For a DNA duplex, $R = 12$ Å and $L = 3.4N$ Å, where N is the number of base pairs.

The general theory for the spin response in CW EPR shows that the line shape is a complicated function of the dynamics, which enter mathematically in terms of the Fourier transforms of correlation functions of orientation-dependent terms in the spin Hamiltonian. Therefore, a consideration of the correlation functions, and associated correlation times, provides insight into the sensitivity of the line shape to dynamics.

In the present case a spin label is covalently attached to a base pair, specifically the jth base pair, where $1 \leq j \leq N$. The base pair is embedded in the molecule. The molecule is free to tumble in solution. A series of Euler angles then is needed to connect the spin label to the laboratory frame. Let ϕ be the rotation to the molecule and ϕ_j be the rotation to the jth base pair. These two rotations are connected by the relative rotation, ϵ_j. The spin label is related to the jth base pair by the Euler angles, ϵ_L. The spin label may be found directly in the laboratory by Euler angles ϕ_L.

The relevant correlation functions directly related to the line shape are those for the spin label: The dependence of the spin Hamiltonian on orientation is given by Wigner rotational matrix elements of the form $D^l_{mn}(\phi_L)$ where $l = 2$ and $n = 0$ for secular terms and $n = \pm 1$ for pseudosecular terms. The m index runs from $-l$ to $+l$. First, however, let us consider the correlation functions for the jth base pair. The correlation function, as an autocorrelation of the Wigner rotational matrix elements, $D^l_{mn}(\phi_j)$, is defined as

$$\rho^l_m(t) = (2l + 1)\langle D^{l*}_{mn}[\phi_j(t)] D^l_{mn}[\phi_j(0)]\rangle \quad \text{(A-3A)}$$

In the applications considered here the correlation function will not depend on the n index. All cross-correlation functions vanish, and are therefore not considered here. The associated correlation time is defined as

$$\tau^l_m = \int_0^\infty \rho^l_m(t)\, dt \quad \text{(A-3B)}$$

When $\rho^l_m(t)$ is a simple exponential decay, then the correlation time τ^l_m is the decay time of the exponential.

The simplest picture of the motions of a base pair is that of the DNA being a totally rigid object and therefore the base moves only as the overall molecules moves, and the coordinates in the base can be taken to be coincident with those of the entire molecule. Since the persistence length of DNA is on the order of 600 Å, DNAs of short length ($N < 30$) will nearly fulfill this condition. Duplex DNAs of longer length will be expected to deviate from the assumption of single body motion. The correlation functions for a rigid object of cylindrical symmetry are known:

$$\rho^l_m(t) = e^{-\lambda^l_{mn} t} \quad \text{(A-4A)}$$

where

$$\lambda^l_{mn} = D_{\text{perp}} l(l + 1) + (D_{\text{para}} - D_{\text{perp}}) m^2 \quad \text{(A-4B)}$$

The associated correlation times are

$$\tau^l_m = (\lambda^l_{mn})^{-1} \quad \text{(A-4C)}$$

The correlation function for the case of a weakly bending and twisting rod have also been evaluated (Wu et al., 1987) and are given approximately as

$$\rho^l_m(t) = e^{-\lambda^l_{mn} t} e^{-a^l_{mn}(j)} \quad \text{(A-5A)}$$

In this case the correlation times are

$$\tau^l_m = (\lambda^l_{mn})^{-1} e^{-a^l_{mn}(j)} \quad \text{(A-5B)}$$

Note that the correlation times for the jth base pair depend on the location of that base pair in the molecule. The $a^l_{mn}(j)$ which depend on the amount of twist and flex have been evaluated elsewhere (Wu et al., 1987). The greater the twist and/or flex the larger $a^l_{mn}(j)$, and the τ^l_m becomes smaller, and smaller correlation times represent faster motion.

For the case of a base pair in the middle ($j = N/2$)

$$a^l_{mn}(N/2) \cong [l(l + 1) - m^2]\frac{L}{12P} + m^2\frac{k_B T N}{12\alpha}$$

where $L = 3.4N$ is the contour length, P is the dynamic persistence length, and α is the Hookean twisting force constant. Assuming that the force constants for twist and flex are approximately the same leads to

$$a^l_{mn}(N/2) \simeq l(l + 1)L/12P$$

We now consider the correlation function for the spin label:

$$\rho'^l_m(t) = (2l + 1)\langle D^{l*}_{mn}[\phi_L(t)] D^l_{mn}[\phi_L(0)]\rangle$$

and

$$\tau'^l_m = \int_0^\infty \rho'^l_m(t)\, dt$$

Since the Euler angles are coupled by an internal rotation of ϵ_L, the Wigner rotation matrix elements are related:

$$D^l_{mn}(\phi_L) = \sum_{s=-l}^{+l} D^l_{ms}(\epsilon_L) D^l_{sn}(\phi_j)$$

Then

$$\rho'^l_m(t) = \sum_{s,s'} (2l + 1)\langle D^{l*}_{ms}[\epsilon_L(t)] D^{l*}_{sn}[\phi_j(t)] D^l_{ms'}[\epsilon_L(0)] D^l_{s'n}[\phi_j(0)]\rangle$$

Since the motion of the probe, relative to the base pair, is independent of the motion of the base pair:

$$\rho'^l_m(t) = \sum_{s,s'} (2l + 1)\langle D^{l*}_{sn}[\phi_j(t)] D^l_{s'n}[\phi_j(0)]\rangle \langle D^{l*}_{ms}[\epsilon_L(t)] D^l_{ms'}[\epsilon_L(0)]\rangle$$

For the sake of simplicity we assume that the spin label is rigidly attached to the base pair. The above formulation shows that if this is not the case then the effect of local base-independent probe mobility on the correlation times can be considered. Assuming a rigidly coupled spin probe means that ϵ_L is not a function of time and therefore

$$\rho'^l_m(t) = \sum_{s,s'} D^{l*}_{ms}(\epsilon_L) D^l_{ms'}(\epsilon_L)(2l + 1)\langle D^{l*}_{sn}[\phi_j(t)] D^l_{s'n}[\phi_j(0)]\rangle$$

The dynamic averaging over the base-pair motion has been evaluated in eq A-3 and A-4. The Wigner matrix elements do not cross-correlate; therefore the cases where $s \neq s'$ all vanish:

$$\tau'^l_m = \sum_{s=-l}^{+l} |D^l_{ms}(\epsilon_L)|^2 \tau^l_s \quad \text{(A-6)}$$

This result shows that the correlation times for the spin label are simple linear combinations of the correlation times for the base pair. Since $\sum_s |D^l_{ms}(\epsilon_L)|^2 = 1$, the Wigner rotational matrix elements act as weights for the relative contributions of the correlation times for the base pair to the correlation times of the probe. Therefore an estimate of the maximum and minimum values of τ^l_m will give a range within which the τ'^l_m will be found. Therefore we evaluate τ^l_m for specific cases.

From the equation for the eigenvalues and for the case of $l = 2$, the usual dipolar term

$$\tau_m^2 = \frac{1}{\lambda_{m,0}^2} = \frac{1}{6D_{\text{perp}} + m^2(D_{\text{para}} - D_{\text{perp}})} \quad \text{(A-7)}$$

Then for duplex DNAs of specific numbers of base pairs at 0 °C

no. of base pairs of duplex DNA	$\tau_\perp = 1/6D_{\text{perp}}$	$\tau_\parallel = 1/6D_{\text{para}}$	τ_0^2	$\tau_{\pm 1}^2$	$\tau_{\pm 2}^2$
12	14.3	7.5	14.3	12.4	8.9
24	54.5	13.3	54.5	35.9	17.8
150	4503.3	72.3	4503.3	401.3	107.5

D_{perp} and D_{para} are evaluated according to eq A-1A and A-1B. The values of all the parameters and constants needed to evaluate D_{perp} and D_{para} are contained in the text of this appendix. τ_m^2 is evaluated according to eq A-7. All the values are given in nanoseconds. Therefore any characteristic rotational correlation time, τ_c, for the spin label must be within the range spanned by these values, regardless of the tilt angle, ϵ_L. In the case of the dodecamer, for example, the time range of τ_c is 9–14 ns.

While $1/6D_{\text{perp}}$ and $1/6D_{\text{para}}$ bear no direct relation to any physical observable, they have been defined by Mason et al. (1974) as $\tau_\perp$ and $\tau_\parallel$, respectively. It is shown above that τ_0^2 and $\tau_{\pm 2}^2$ bracket the effective time, τ_c, that can be observed by the spin probe. τ_0^2 corresponds to the autocorrelation of $D_{0,0}^2(\Omega) = (3\cos^2\theta - 1)/2$ and hence measures the rotational rate perpendicular to the helix axis. $\tau_{\pm 2}^2$ corresponds to the autocorrelation of $D_{\pm 20}^2(\Omega) = (^3/_8)^{1/2}\sin^2\theta e^{\pm i2\phi}$ and hence measures the rotational rate about the helix axis. When the tilt angle, ϵ_L, equals 0, then the probe and molecular frames are coincident: $|D_{m,s}^l(0)|^2 = \delta_{m,s}$. In this case $\tau_0'^2 = \tau_0^2 = 1/6D_{\text{perp}} = \tau_\perp$ and $\tau_{\pm 2}'^2 = \tau_{\pm 2}^2 = 1/(2D_{\text{perp}} + 4D_{\text{para}}) = \tau_\parallel/[^2/_3 + {}^1/_3(\tau_\parallel/\tau_\perp)]$.

In summary then, for a rigid object the size of DNA, τ_2^2 and τ_0^2 represent the characteristic correlation times for rotation around and perpendicular to the axis of cylindrical symmetry, respectively. The effective characteristic rotational time, τ_c, as observed by the spin probe, will be bounded by these two correlation times. This will hold, regardless of the tilt angle, ϵ_L.

The time $\tau_\parallel$ and $\tau_\perp$, reported by Kao et al. (1983) for their spin-labeled DNA, were obtained by optimizing the fit of the simulated to the experimental line shape, assuming rigid-body, anisotropic motion as the appropriate model for the probe's molecular dynamics. Their reported values for $\tau_\parallel$ and $\tau_\perp$ were both much faster than those computed here and were interpreted in terms of rapid local motion and helix axis motion. We have computed the quantities $\tau_\parallel$ and $\tau_\perp$ and the closely related correlation times τ_m^2 for a rigid object the size of DNA predicted by hydrodynamic theory and find it most encouraging that for the spin probe reported in this work the experimentally obtained values of τ_c lie between τ_0^2 (closely related to $\tau_\perp$) and $\tau_{\pm 2}^2$ (closely related to $\tau_\parallel$). We have also shown how internal flexibility of the base pairs and of the probe, moving independently of the base pairs, may be considered. At this level of analysis there is no need to consider directly the internal flexibility of the probe. If such flexibility exists, it is of very limited amplitude and has been subsumed by the choice of effective tensors.

References

Aboul-ela, F., Koh, D., & Tinoco, I., Jr. (1985) *Nucleic Acids Res. 13*, 4811–4824.

Allison, S. A., & Schurr, J. M. (1979) *Chem. Phys. 41*, 35–59.

Anderson, J. E., Ptashne, M., & Harrison, S. C. (1987) *Nature 326*, 846–852.

Ashikawa, I., Kinosita, K., & Ikegami, A. (1984) *Biochim. Biophys. Acta 782*, 87–93.

Atkinson, T., & Smith, M. (1985) in *Oligonucleotide Synthesis* (Gait, M. J., Ed.) pp 35–45, IRC Press, Oxford.

Barkley, M. D., & Zimm, B. H. (1979) *J. Chem. Phys. 70*, 2991–3007.

Beaucage, S. L., & Caruthers, M. H. (1981) *Tetrahedron Lett. 22*, 1859–1862.

Bobst, A. M., Kao, S.-C., Toppin, R. C., Ireland, J. C., & Thomas, I. E. (1984) *J. Mol. Biol. 173*, 63–72.

Bobst, A. M., Pauly, G. T., Keyes, R. S., & Bobst, E. V. (1988) *FEBS Lett. 228*, 33–36.

Bolton, P. H., & James, T. L. (1980) *J. Am. Chem. Soc. 102*, 25–31.

Brown, T., Hunter, W. N., Kneale, G., & Kennard, O. (1986) *Proc. Natl. Acad. Sci. U.S.A. 83*, 2402–2406.

Dickerson, R. E., & Drew, H. R. (1981) *J. Mol. Biol. 149*, 761–786.

Dickerson, R. E., Drew, H. R., Conner, B. N., Wing, R. M., Fratini, A. V., & Kopka, M. L. (1982) *Science (Washington, D.C.) 216*, 475–485.

Dugas, H. (1977) *Acc. Chem. Res. 10*, 47–54.

Early, T. A., & Kearns, D. R. (1979) *Proc. Natl. Acad. Sci. U.S.A. 76*, 4165–4169.

Erie, D., Sinha, N., Olson, W., Jones, R., & Breslauer, K. (1987) *Biochemistry 26*, 7150–7159.

Hare, D. R., Wemmer, D. W., Chou, S.-H., Drobny, G., & Reid, B. R. (1983) *J. Mol. Biol. 171*, 319.

Hideg, K., Hankovszky, H. O., Lex, L., & Kulcsar, Gy. (1980) *Synthesis*, 911–914.

Hogan, M. E., & Jardetzky, O. (1979) *Proc. Natl. Acad. Sci. U.S.A. 76*, 6341–6345.

Hogan, M. E., & Austin, R. H. (1987) *Nature (London) 329*, 263–266.

Hunter, W. N., Brown, T., & Kennard, O. (1987a) *Nucleic Acids Res. 15*, 6589–6606.

Hunter, W. N., Brown, T., Kneale, G., Anand, N. N., Rabinovich, D., & Kennard, O. (1987b) *J. Biol. Chem. 262*, 9962–9970.

Kalnik, M. W., Norman, D. G., Zagorski, M. G., Swann, P. F., & Patel, D. J. (1989) *Biochemistry 28*, 294–303.

Kamzolova, S. G., & Postnikova, G. B. (1981) *Q. Rev. Biophys. 14*, 247–288.

Kao, S.-C., & Bobst, A. M. (1985) *Biochemistry 24*, 5465–5469.

Kao, S.-C., Polnaszek, C. F., Toppin, C. R., & Bobst, A. M. (1983) *Biochemistry 22*, 5563–5568.

Koudelka, G. B., Harrison, S. B., & Ptashne, M. (1987) *Nature 326*, 846–852.

Koudelka, G. B., Harbury, P., Harrison, S. C., & Ptashne, M. (1988) *Proc. Natl. Acad. Sci. U.S.A. 85*, 4633–4637.

Kremer, A. B., Mikita, T., & Beardley, G. P. (1987) *Biochemistry 26*, 391–397.

Letzinger, R. L., & Lunsford, W. B. (1976) *J. Am. Chem. Soc. 98*, 3655–3661.

Loeb, A. L., & Kunkel, T. A. (1982) *Annu. Rev. Biochem. 51*, 429–457.

Mailer, C., Danielson, J. D. S., & Robinson, B. H. (1985) *Rev. Sci. Instrum. 56*, 1917–1925.

Mason, R. P., Polnaszek, C. F., & Freed, J. H. (1974) *J. Phys. Chem. 78*, 1324–1329.

Miller, M., Harrison, R. W., Wlodawer, A., Apella, E., & Sussman, J. L. (1988) *Nature 334*, 85–86.

Opella, S. J., Wise, W. B., & DiVerdi, J. A. (1981) *Biochemistry 20*, 284-290.
Pardi, A., Morden, K. M., Patel, D. J., & Tinoco, I., Jr. (1983) *Biochemistry 22*, 1107-1113.
Patel, D. J., Kozlowski, S. A., Ikuta, S., Hakura, K., Bhatt, R., & Hare, D. R. (1982a) *Cold Spring Harbor Symp. Quant. Biol. 471*, 197-206.
Patel, D. J., Kozlwsky, S. A., Marky, L. A., Rice, J. A., Itakura, K., & Breslauer, K. J. (1982b) *Biochemistry 21*, 428-436.
Patel, D. J., Kozlowski, S. A., Marky, L. A., Rice, J. A., Broka, C., Dallas, J., Itakura, K., & Breslauer, K. J. (1982c) *Biochemistry 21*, 437-444.
Pauly, G. T., Thomas, I. E., & Bobst, A. M. (1987) *Biochemistry 26*, 7304-7310.
Redfield, A. G., & Kunz, S. D. (1979) in *NMR and Biochemistry* (Opella, S. J., & Lu, P., Eds.) pp 225-239, Marcel Dekker, New York.
Robins, M. J., & Barr, P. J. (1983) *J. Org. Chem. 48*, 1855-1862.
Robinson, B. H., Lerman, L. S., Beth, A. H., Frisch, H. L., Dalton, L. R., & Auer, L. (1980) *J. Mol. Biol. 139*, 19-44.
Roy, S., Weinstein, S., Borah, B., Nickol, J., Apela, E., Sussman, J. L., Miller, M., Shindo, H., & Cohen, J. S. (1986) *Biochemistry 25*, 7417-7423.
Salisbury, S. A., & Anand, N. N. (1985) *J. Chem. Soc., Chem. Commun.* 985-986.
Seela, F., & Kehne, A. (1987) *Biochemistry 26*, 2232-2238.
Sowers, L. C., Eritja, R., Kaplan, B. E., Goodman, M. F., & Fazakerley, G. V. (1987) *J. Biol. Chem. 262*, 15436-15442.
Spaltenstein, A., Robinson, B. H., & Hopkins, P. B. (1988) *J. Am. Chem. Soc. 110*, 1299-1301.
Spaltenstein, A., Robinson, B. H., & Hopkins, P. B. (1989) *J. Am. Chem. Soc. 111*, 2303-2305.
Streisinger, G., Okada, Y., Emrich, J., Newton, J., Tsugita, A., Terzaghi, E., & Inouye, M. (1966) *Cold Spring Harbor Symp. Quant. Biol. 31*, 77-84.
Thomas, J. C., & Schurr, J. M. (1983) *Biochemistry 22*, 6194-6198.
Thomas, J. C., Schurr, J. M., & Holder, R. D. (1980) *Biopolymers 19*, 1451-1474.
Tirado, M. M., & de la Torre, J.-G. (1980) *J. Chem. Phys. 73*, 1986.
van den Hoogen, Y. T., van Beuzekom, A. A., van den Elst, H., van der Marel, G. A., van Boom, J. H., & Altona, C. (1988) *Nucleic Acids Res. 16*, 2971-2986.
Wahl, P., Paoletti, J., & LePecq, J.-B. (1970) *Proc. Natl. Acad. Sci. U.S.A. 65*, 417-421.
Wemmer, D. E., & Benight, A. S. (1985) *Nucleic Acids Res. 13*, 8611-8620.
Wemmer, D. E., Chou, S. H., Hare, D. R., & Reid, B. R. (1985) *Nucleic Acids Res. 13*, 3755-3772.
Wing, R., Drew, H., Takano, T., Broka, C., Tanaka, S., Itakura, K., & Dickerson, R. E. (1980) *Nature (London) 287*, 755-758.
Wolberger, C., Dong, Y., Ptashne, M., & Harrison, S. C. (1988) *Nature 335*, 789-795.
Wu, P., Fujimoto, B. S., & Schurr, J. M. (1987) *Biopolymers 26*, 1463-1488.

Interaction of Nucleolar Phosphoprotein B23 with Nucleic Acids†

Tamba S. Dumbar,‡ Glenn A. Gentry,§ and Mark O. J. Olson*,‡
Departments of Biochemistry and Microbiology, The University of Mississippi Medical Center, 2500 North State Street, Jackson, Mississippi 39216-4505

Received April 19, 1989; Revised Manuscript Received July 31, 1989

ABSTRACT: The interaction of eukaryotic nucleolar phosphoprotein B23 with nucleic acids was examined by gel retardation and filter binding assays, by fluorescence techniques, and by circular dichroism. All studies utilized protein prepared under native conditions by a newly developed purification procedure. Electrophoretic gel mobility shift assays with phage M13 DNA suggested that protein B23 is a single-stranded nucleic acid binding protein. This was confirmed in competition binding assays with native or heat-denatured linearized plasmid pUC18 DNA where the protein showed a marked preference for the denatured form. In other competition assays, there was no apparent preference for single-stranded synthetic ribo- versus deoxyribonucleotides. Equilibrium binding with poly(riboethenoadenylic acid) indicated cooperative ligand binding with a protein binding site size of 11 nucleotides and an apparent binding constant ($K\omega$) of 5×10^7 M^{-1} which includes an intrinsic binding constant (K) of 6.3×10^4 M^{-1} and a cooperativity factor (ω) of 800. In circular dichroism (CD) studies, protein B23, when combined with the single-stranded synthetic nucleic acids poly(rA) and poly(rC), effected a decrease in ellipticity and a shift of the positive peak at 260-270 nm toward higher wavelengths, indicating helix destabilizing activity. No CD changes were seen with double-stranded poly(dA·dT). The change in ellipticity of poly(rA) was sigmoidal upon addition of protein, confirming the cooperative behavior seen with fluorescence methods. These studies indicate that protein B23 binds cooperatively with high affinity for single-stranded nucleic acids and exhibits RNA helix destabilizing activity. These features may be related to its role in ribosome assembly.

Phosphoprotein B23 (M_r/pI = 38K/5.1) is a eukaryotic RNA-associated nucleolar protein whose sequence has been recently determined in several species including rat (Chang et al., 1988), mouse (Schmidt-Zachmann et al., 1988), human (Chan et al., 1989), and *Xenopus laevis* (NO38) (Schmidt-Zachmann et al., 1987). The close association of the protein with RNA is suggested by the fact that it is localized to the granular region of the nucleolus (Ochs et al., 1983; Michalik

† This work was supported in part by NIH Grants GM28349 and RR05386 (to M.O.J.O.).
‡ Department of Biochemistry.
§ Department of Microbiology.

0006-2960/89/0428-9495$01.50/0